for example, through steric effects (which will increase the Q_C contribution) via the presence of bulky groups at the terminal allylic methylene centers and thus force a synchronous mechanism.

Second, the surface topology is influenced strongly by the long-bond interaction K_{14}. We have shown that if the long-bond interaction K_{14} is turned off, the biradical region disappears. Thus, the presence of a substituent at sites 1 or 4 that enhances this effect will force a biradicaloid mechanism. Dewar and Wade[10] have shown that phenyl substitution at the positions 1 and 4 increases the rate by a factor of 2000, in agreement with this observation.

Registry No. 1,5-Hexadiene, 592-42-7.

Mechanism of Ground-State-Forbidden Photochemical Pericyclic Reactions: Evidence for Real Conical Intersections

Fernando Bernardi,*[1a] Sushovan De,[1b] Massimo Olivucci,[1b] and Michael A. Robb*[1b]

Contribution from the Dipartimento di Chimica, "G. Ciamician", dell'Universita di Bologna, Via Selmi 2, 40126 Bologna, Italy, and the Department of Chemistry, King's College, London, Strand, London WC2R 2LS, U.K. *Received May 31, 1989*

Abstract: The presence of a conical intersection between the S_0 and S_1 surfaces for ground-state-forbidden photochemical pericyclic reactions is demonstrated by using results from an effective (valence bond) Hamiltonian and MC-SCF computations. The existence of such topological features is an important feature in the mechanism since it permits a fully efficient return to S_0 from the S_1 excited state. An example is presented for the 2 + 2 cycloaddition reaction of two ethylene molecules and the electrocyclic reaction of *cis*-butadiene.

I. Introduction

Pericyclic reactions, which are ground-state-forbidden (in the Woodward–Hoffmann scheme), are assumed to be excited-state-allowed in S_1 because the surface topology of S_1 is assumed to possess a minimum that corresponds to a diradicaloid structure that has approximately the same geometry as the "antiaromatic" transition state on S_0. Thus, the central feature in the mechanism of an excited-state pericyclic reaction is usually assumed to be the existence of suitable surface crossing (a funnel) that allows for the occurrence of a radiationless jump from S_1 to S_0. (For a good discussion of these points the reader is referred to ref 2 and 3). The decay probability P from S_1 to S_0 can be approximated by the Landau Zener formula (see the discussion of Salem[3] or Tully and Preston[4]):

$$P = \exp -\pi^2 g^2 / h\nu\, \delta s \qquad (1)$$

where ν is the nuclear velocity along the reaction coordinate, g is the energy gap at the avoided crossing, and δs is the difference in slopes between the intersecting "diabatic" states. Clearly, the larger the value of g the smaller is P. The surfaces S_1 and S_0 are assumed to avoid each other and it is this gap g that controls this reaction.

In contrast to the preceding discussion, if the S_0 and S_1 states actually touch at the funnel geometry (in a conical intersection[5]), the return to S_0 will be fully efficient since the return to S_0 occurs as soon as the funnel is reached. As a consequence, the rate of the reaction will not be controlled by the gap g between the S_0 and S_1 surfaces but will be controlled by the usual topological features of either the ground- or excited-state surfaces (e.g., a transition state arising from an S_1/S_2 avoided crossing on the excited surface). It is widely recognized that such conical intersections do frequently occur, and the purpose of this article is to demonstrate this for two "textbook" pericyclic reactions, the 2 + 2 cycloaddition of two ethylene molecules and the electrocyclic ring closure of *cis*-butadiene.

Scheme I

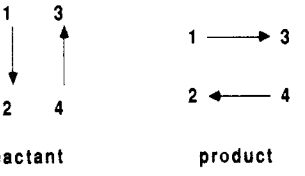

Recently, we have shown[6] how an MC-SCF wave function can be transformed to valence bond (VB) space. (For a discussion of VB theory as used in this paper, the reader is referred to ref 7 and 8.) We now give a simple discussion of how such a conical intersection can arise in the language of VB theory and then demonstrate using the methods discussed in ref 6 that such a topological feature actually arises for the two reactions.

We shall illustrate our discussion using the classical example of the 2 + 2 reaction of two ethylene molecules. In VB theory we can represent (at the simplest level) the ground and "valence" excited states of two ethylene molecules using two VB structures characteristic of the spin coupling of the reactant and products as shown in Scheme I. Using a two-level secular equation, taking one reference wave function as the reactant and the other as the

(1) (a) Dipartimento G. Ciamician, dell'Universita di Bologna. (b) King's College, London.

(2) (a) Turro, N. J. *Modern Molecular Photochemistry*; Benjamin Publishing: Reading, MA, 1978. (b) Michl, J.; Bonacic-Kotecky, V. *Electronic Aspects of Organic Photochemistry*; Wiley, New York, 1989.

(3) Salem, L. *Electrons in Chemical Reactions: First Principles*; Wiley, New York, 1982.

(4) Tully, J. C.; Preston, R. K. *J. Am. Chem. Soc.* **1971**, *55*, 562.

(5) (a) Von Neumann, J.; Wigner, E. *Phys. Z.* **1929**, *30*, 467. (b) Teller, E. *J. Phys. Chem.* **1937**, *41*, 109. (c) Herzberg, G.; Longuet-Higgins, H. C. *Trans. Faraday Soc.* **1963**, *35*, 77. (d) Herzberg, G. *The Electronic Spectra of Polyatomic Molecules*; Van Nostrand: Princeton, NJ, 1966, p 442. (e) Mead, C. A.; Truhlar, D. G. *J. Chem. Phys.* **1979**, *70*, 2284. (f) Mead, C. A. *Chem. Phys.* **1980**, *49*, 23. (g) Keating, S. P.; Mead, C. A. *J. Chem. Phys.* **1985**, *82*, 5102. (h) Keating, S. P.; Mead, C. A. *J. Chem. Phys.* **1987**, *86*, 2152.

(6) Bernardi, F.; Olivucci, M.; McDouall, J. J. W.; Robb, M. A. *J. Chem. Phys.* **1988**, *89*, 6365.

(7) McWeeny, R.; Sutcliffe, B. *Methods of Quantum Mechanics*; Academic: New York, 1969.

(8) Eyring, H.; Walter, J.; Kimball, G. *Quantum Chemistry*; Wiley: New York, 1944.

0002-7863/90/1512-1737$02.50/0

product, we can find the ground- and excited-state wave functions as a linear combination of these reactant and product structures through the solution of the usual secular equation

$$\begin{pmatrix} \alpha_R - E^i & \beta \\ \beta & \alpha_P - E^i \end{pmatrix} \begin{pmatrix} C_R^i \\ C_P^i \end{pmatrix} = 0 \tag{2}$$

The matrix elements can be written symbolically as

$\alpha_R =$ 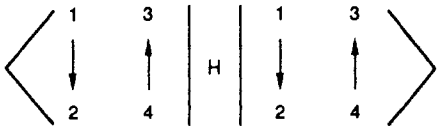 (3a)

$\alpha_P =$ 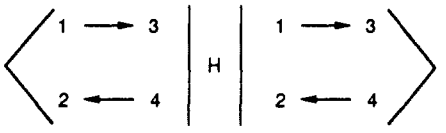 (3b)

$\beta =$ 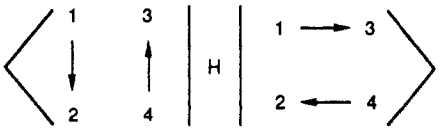 (4)

Similarly the wave function has the form

$\Psi^i = C_R^i$ 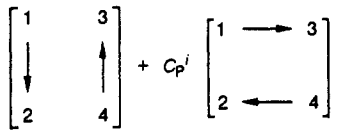 (5)

The precise form of the expressions for α_R, α_P, and β depends upon the details of the orthogonalization of the spin functions and are given in ref 6. In general, these quantities can always be expressed in the form

$$\alpha_R = Q + K \tag{6a}$$

$$\alpha_P = Q - K \tag{6b}$$

The quantity α_R is the "diabatic" energy of the reactant configuration and α_P is the "diabatic" energy of the product configuration. Thus, α_R coincides with the reactant energies at the reactant geometries and α_P coincides with the product energies at the product geometries. The term Q is the Coulomb energy and includes the nonbonded repulsions (plus nuclear–nuclear repulsions) in addition to the nuclear–electron attraction and electron–electron repulsion of the valence electrons. We shall refer to K as the "bond exchange". The quantity β is the resonance energy.

We can now easily give the conditions for a conical intersection. The eigenvalues of eq 2 are

$$E = Q \pm T \tag{7}$$

where we refer to T as the total exchange energy, which we can write as

$$T = (K^2 + \beta^2)^{1/2} \tag{8}$$

While the precise form of K and β depends upon the details of the choice of spin functions;[6] T is always given by the following expression for four orbitals and four electrons:

$$T = \{(K_P - K_X)(K_R - K_X) + (K_P - K_R)^2\}^{1/2} \tag{9}$$

The term K_P is the exchange energy of the products ($K_{13} + K_{24}$), K_R is the exchange energy of the reactants ($K_{12} + K_{34}$), and K_X is the nonbonded exchange energy ($K_{14} + K_{23}$). Obviously the condition for the excited-state and ground-state intersection ($T = 0$ from eq 7) can either be stated as (from eq 9)

$$K_P - K_R = 0 \tag{10a}$$

$$K_R - K_X = 0 = K_P - K_X \tag{10b}$$

or more conventionally as (from eq 8)

$$K = 0 \quad \text{(i.e., } \alpha_R = \alpha_P\text{)} \tag{11a}$$

$$\beta = 0 \tag{11b}$$

The noncrossing rule between states of the same symmetry in one dimension (diatomic molecules) was first proved by von Neumann and Wigner.[5a] It was extended to polyatomic molecules (conical intersections) by Teller[5b] and subsequently Herzberg and Longuet-Higgins[5c] derived the conditions for nonsymmetrical systems (see also ref 5d). More recently, the problem of conical intersections has been treated in a very general way.[5e,f] A conical intersection may occur easily if one of the conditions, $\beta = 0$, is fulfilled because the two levels have different symmetry. If the symmetry of the two levels is the same (as in the case under consideration) the occurrence of a conical intersection might be expected to be rare; however, this is not the case. Salem[3] gives a good discussion for the case of a three-orbital system using the analogue of eq 10. Conical intersections are well-known at large interfragment distances (e.g., the well-known triatomic case $O(^3P) + H_2(^3\Sigma_g^+)$ with $O(^1D) + H_2(^1\Sigma_g^+)$,[5d] where β goes to zero simply because of the large interfragment distance. Davidson and co-workers[9] studied conical intersections for variety of chemical systems (NO_2,[9a] H_3, HCO, CH_2, and NO_2,[9b] 1,3-dimethylenecyclobutadiene,[9c] and HCO_2[9d]). As we shall now demonstrate, for four orbitals and four electrons, the conditions of eq 10 may be quite easy to satisfy at "normal" interatomic distances characteristic of the geometry of the "antiaromatic" transition state on S_0. Thus it may turn out that this feature is a common occurrence in the mechanisms of organic photochemistry. Of course the double cone is represented in the space of two geometric variables; but the potential energy functions depend on other variables and the intersection occurs for any values of these variables. Thus two n dimensional surfaces would intersect along an $n - 2$ dimensional hyperline.

As we have discussed in detail elsewhere,[6] it is possible to project an MC-SCF wave function onto the space of the two VB structures shown in Scheme I via the construction of an effective Hamiltonian. The numerical values of the exchange integrals K_{ij} that occur in the preceding discussion can be obtained from this effective Hamiltonian. The behavior of the exchange integrals K_{ij} can be rationalized by using the Heitler–London expression for two electrons:

$$K_{ij} = [ij|ij] + 2s_{ij}\langle i|h|j\rangle \tag{12}$$

where $[ij|ij]$ is the usual two-electron-exchange repulsion integral, $\langle i|h|j\rangle$ is the one-electron-exchange integral (nuclear electron attraction), and s_{ij} is the overlap integral between orbitals i and j. K_{ij} will be dominated by the attraction term. These exchange integrals are simple functions of the distance between the reactive sites i and j by virtue of s_{ij}. Given this fact, it remains to illustrate that the condition for conical intersection given in eq 10 is easily satisfied in practice.

II. The 2 + 2 Reaction of Two Ethylene Molecules

In ref 10 we have presented the results of MC-SCF computations for the various critical points that are important for the ground-state 2 + 2 cycloaddition of two ethylene molecules. In this work we characterized the antiaromatic "transition state" with D_{2h} symmetry for the $_2s + _2s$ forbidden reaction. This "transition state" was found to be a local maximum with two negative directions of curvature. In subsequent work, on searching the S_1 surface in this region, we find the expected D_{2h} diradicaloid structure that has a geometry that is very similar to the antiaromatic S_0 structure. However, this structure is not a minimum but rather is a transition state. The negative direction of curvature in this S_1 transition structure corresponds to a nontotally symmetric

(9) (a) Jackels, C. F.; Davidson, E. R. *J. Chem. Phys.* **1976**, *64*, 2908. (b) Davidson, E. R. *J. Am. Chem. Soc.* **1977**, *99*, 397. (c) Davidson, E. R.; Borden, W. T.; Smith, J. *J. Am. Chem. Soc.* **1978**, *100*, 3299. (d) Feller, D.; Huyser, E. S.; Borden, W. T.; Davidson, E. R. *J. Am. Chem. Soc.* **1983**, *105*, 1459.

(10) Bernardi, F.; Bottoni, A.; Robb, M. A.; Schlegel, H. B.; Tonachini, G. *J. Am. Chem. Soc.* **1985**, *107*, 2260–2264.

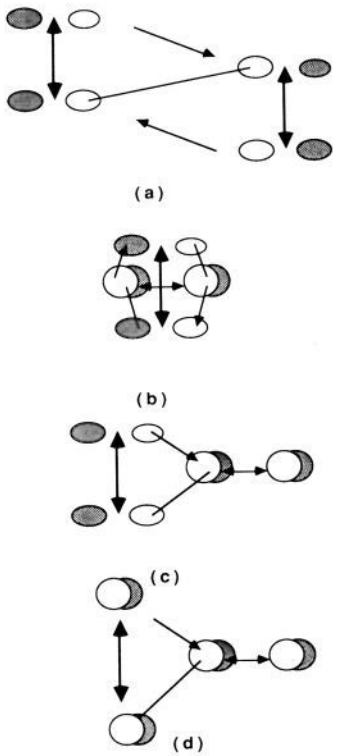

Figure 1. Schematic representation of possible geometries on the $n - 2$ hyperline where the conical intersection condition given in eq 11a,b may be satisfied. The double-headed arrows represent K_R, the single-headed arrows represent K_P, and the lines with no arrows represent K_X contributions.

Scheme II

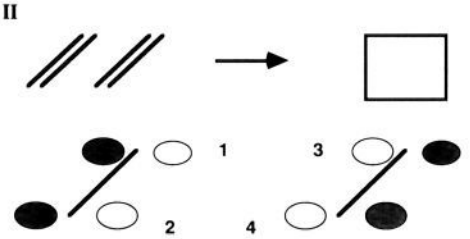

distortion and would indicate the presence of a minimum with a trapezoidal geometry of C_{2h} symmetry. We now proceed to demonstrate that motion along this coordinate leads not to a minimum but rather to a conical intersection with S_0.

For the 2 + 2 reaction of two ethylene molecules, the four active orbitals are the p^π orbitals of the ethylenic fragments as shown in Scheme II. Clearly the exchange integrals in K_R will decrease rapidly as the intrafragment CC distance is increased because the "sideways" overlap between the p^π orbitals decreases. The exchange integrals in K_P will increase rapidly as the interfragment CC distance is decreased because the "end-on" σ-type overlap of the p^π orbitals increases. The K_X integrals will be quite small for rectangular geometries so that while one might satisfy $K_P - K_R = 0$ at the rectangular geometry of an assumed "antiaromatic" transition state of S_0, the condition $K_R - K_X = 0$ can never be satisfied for such a geometry.

It remains to postulate possible geometries where one might satisfy simultaneously the two conditions given in eq 10. Several possibilities suggest themselves immediately and these are given schematically on Figure 1. Here we have indicated the contributions to K_R by double-headed arrows, to K_P by single-headed arrows, and to K_X by simple lines. Each of the structures corresponds to a situation where $K_P = K_X$. The condition would then be satisfied when the intrafragment CC distance was changed so that $K_R = K_P$.

Of course all of the structures shown probably lie on the same or on different $n - 2$ dimensional surfaces where the conditions

Chart I

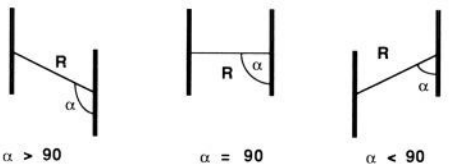

10/11 are satisfied. However, when the conditions 10/11 are satisfied, then the energy of ground and excited states is merely equal to Q, the Coulomb energy. Thus, we are interested in the lowest energy point on one of the possible $n - 2$ dimensional surfaces. The behavior of Q is quasi-classical. On the one hand we must have small electrostatic contributions from the active orbitals of the form

$$J_{ij} = [ii|jj] + \langle i|h|i\rangle + \langle j|h|j\rangle$$

which will be dominated by the nuclear attraction terms in $\langle i|h|i\rangle$ at large interfragment separation and by the two-electron repulsion integrals at small interfragment distance. On the other hand we also have quasi-classical contributions from the repulsions arising from the closed-shell core, from angle strain, and from dipole–dipole interactions, which will dominate Q at small interfragment separation. Thus, for the 2 + 2 cycloaddition, Q will be very repulsive in the region of structures 1b through 1d (Figure 1) because of the methylene H atoms. Thus, if there is an interesting region of conical intersection for the 2 + 2 cycloaddition, it should be found in the region of structure 1a.

To be completely rigorous, in order to locate the lowest energy point on the surface where the conditions 10/11 are satisfied we must perform a complicated geometry optimization. One must do a constrained optimization where one minimizes the energy (which will just be Q) subject to the constraint that eq 10 or 11 is satisfied. We are currently developing such optimization methods. However, our present objective is simply to demonstrate that the conical intersection exists at an energy that is accessible.

We now present evidence for the existence of a conical intersection in the region of the structure shown schematically in Figure 1a. Our evidence will be presented by computing the energy on a grid of points in a subspace that consists of the interfragment CC distance and an internal coordinate that connects the rectangular $2_s + 2_s$ S_0 transition state with the trans fragmentation transition state, as shown in Chart I. (The optimized geometries of these states are to be found in ref 10.) The potential surfaces are obtained in two different ways. Firstly a global view of the surface is obtained by fitting the Coulomb and exchange parameters obtained from an MC-SCF effective Hamiltonian calculation to simple functions of the interatomic distances and computing the energy on a large grid through solution of eq 7 and 9. This approach enables us to display the geometrical behavior of eq 10 or 11. As a rigorous test that is independent of any errors associated with fitting methods, we have computed a small grid of points, using MC-SCF theory, in the region of the apex of the double cone at STO 3G and 4-31G basis sets.

The fitted potential energy surfaces for the ground and excited states are shown in Figures 2 and 3. The X axis (top left to bottom right) corresponds to the variable R. The Y axis (bottom left to top right) corresponds to the variable α and is defined in Chart I. The intrafragment CC distance has been interpolated as a function of R. In order to orient the reader, it is useful to note that the middle value of the variable α is 90° so that the $2_s + 2_s$ S_0 reaction path runs diagonally from right to left through the middle of the figure with the reactants on the right and the well on the left corresponding to the product region. There are two asynchronous "channels" on either side of the $2_s + 2_s$ S_0 reaction path that correspond to the ground-state nonconcerted (trans) pathway. The bottom part of the double cone that lies between the $2_s + 2_s$ S_0 reaction path and the asynchronous channels is clearly evident. In Figure 3 the excited-state surface shows the other half of the double cone. Notice that the critical point (grid point $X = 11$, $Y = 21$) that lies above the ground-state $2_s + 2_s$

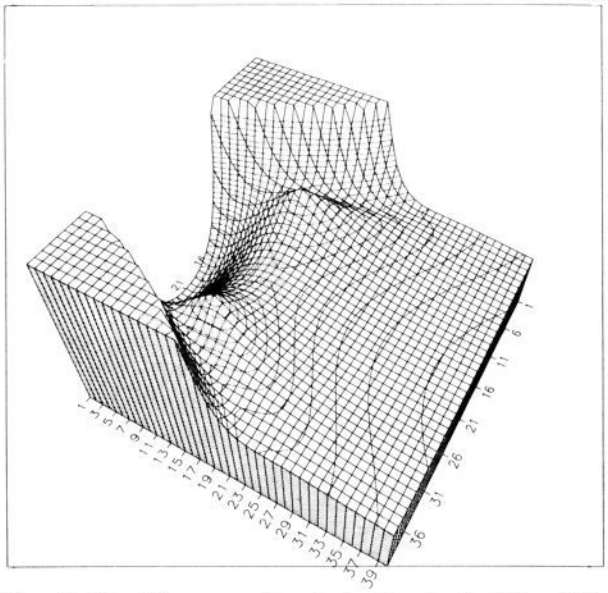

Figure 2. Potential energy surface obtained by using the VB model for the ground-state (S_0) 2 + 2 cycloaddition of two ethylene molecules. The X axis (diagonal top left to bottom right) is the interfragment distance R and as Y axis (diagonal top right to bottom left) the angle α defined in Scheme II. Each division on the X axis corresponds to an increment of $0.1a_0$ (0.053 Å) and the first division corresponds to $R = 3.0a_0$ (1.58 Å). Each division on the Y axis corresponds to an increment of 3.5° and the first division corresponds to $\alpha = 20°$. The values of the remaining geometrical parameters have been interpolated with respect to R.

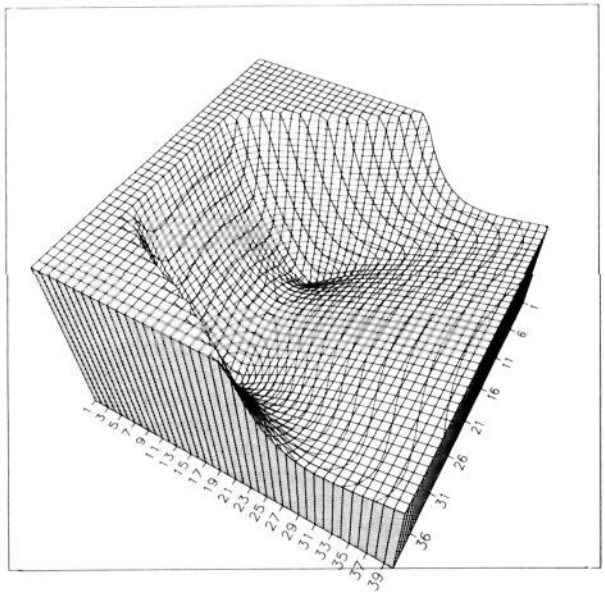

Figure 3. Potential energy surface obtained by using the VB model for the excited-state (S_1) 2 + 2 cycloaddition of two ethylene molecules. The X and Y axes are defined as in Figure 2.

S_0 transition state is itself a transition state, and as we have already pointed out, this feature has been confirmed by geometry optimization with analytical Hessian computation at STO 3G and 4-31G levels. The transition vector (corresponding to the negative direction of curvature) points to the conical intersection at grid point $X = 11$, $Y = 33$. In Figure 4 we plot $-T$ as defined in eq 9. The condition of eq 10 shows as a spike in this surface. Finally in Figure 5, we give the surface of the lowest energy sheet of α_R and α_P as defined in eq 6a/6b. The ridge in this figure corresponds to the locus of points that satisfy the condition of eq 11a. (The ridge appears a little ragged in the figure. This is due to the finite numerical accuracy used in the computation and has no physical significance.) In Figure 6 we show the corresponding surface for

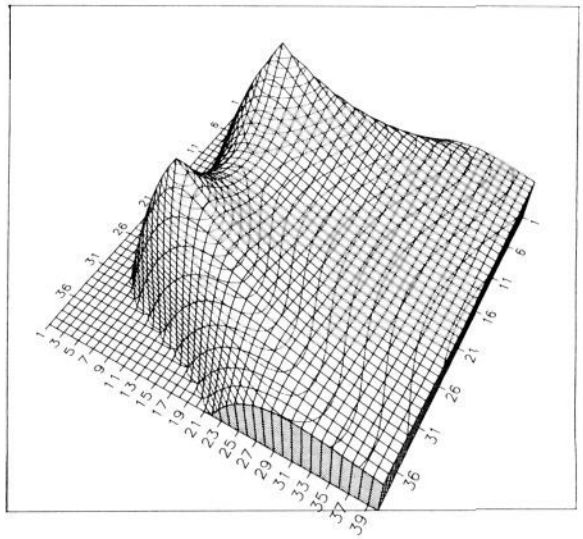

Figure 4. Potential energy surface of $-T$ (eq 9) obtained by using the VB model for the 2 + 2 cycloaddition of two ethylene molecules. The X and Y axes are defined as in Figure 2.

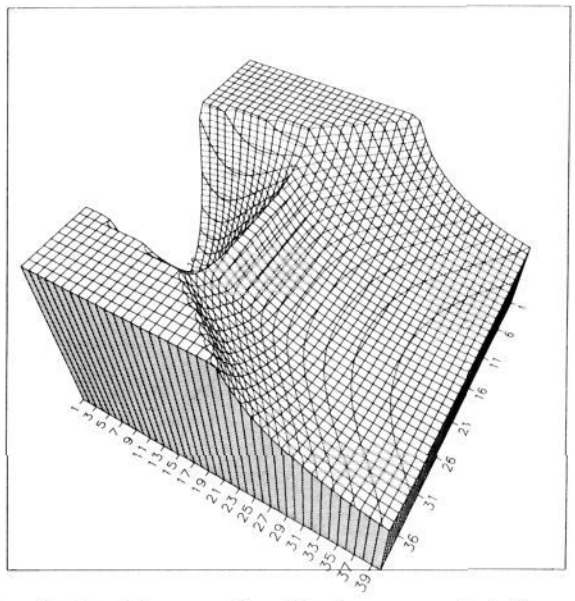

Figure 5. Potential energy surface of the lowest energy sheet of α_R and α_P as defined in eq 6a/6b obtained by using the VB model for the 2 + 2 cycloaddition of two ethylene molecules. The ridge in this figure corresponds to the locus of points that satisfy the condition of eq 11a. The X and Y axes are defined as in Figure 2.

$|\beta|$, the resonance energy. Here the valley corresponds to the condition of eq 11b. Notice that the intersection of the ridge of Figure 5 and the valley of Figure 6 correspond to conditions of eq 11a and b holding simultaneously and occurs at the geometry of the double cone in Figures 2 and 3.

Finally, the ground-state surface for the double cone computed at the MC-SCF level is given in Figures 7 and 8 and confirms the existence of this topological feature. The geometry of the apex of the cone at the 4-31G level estimated from the grid is given in Figure 9 (only the values of R and α are optimized; the remaining parameters are those of the ground-state $2_s + 2_s$ S_0 D_{2h} transition state). Of course the apex of the cone is not as sharp in Figures 7 and 8 as in the fitted surfaces of Figures 2 and 3 because (a) the geometry of the remaining variables has not been interpolated and (b) for reasons of economy we have only used a 6 × 6 grid in each case. Nevertheless, the existence of the conical intersection is confirmed. Any attempt to perform a geometry optimization in this region fails completely because we have a true

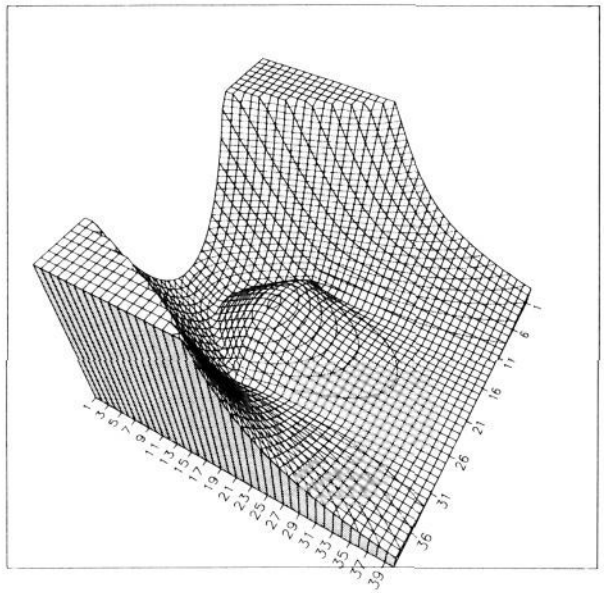

Figure 6. Potential energy surface for $|\beta|$, the resonance energy, obtained by using the VB model for the 2 + 2 cycloaddition of two ethylene molecules. The valley corresponds to the condition of eq 11b, and the intersection of the ridge of Figure 5 and the valley of this figure corresponds to conditions of eq 11a and b holding simultaneously and occurs at the geometry of the double cone in Figures 2 and 3. The X and Y axes are defined as in Figure 2.

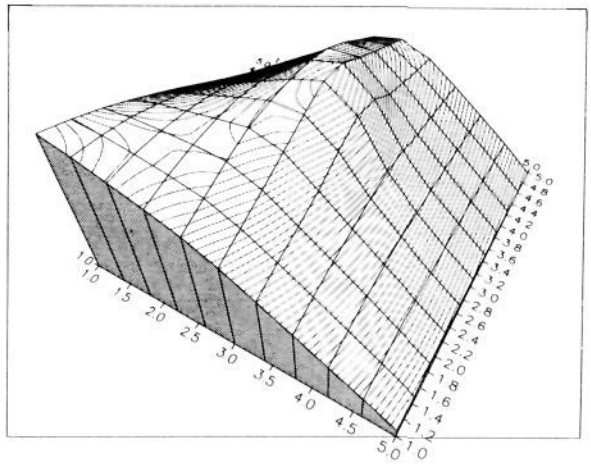

Figure 7. Potential energy surface obtained by using the MC-SCF method at the STO 3G level for the ground-state (S_0) 2 + 2 cycloaddition of two ethylene molecules. The X axis (diagonal top left to bottom right) is the interfragment distance R and as Y axis (diagonal top right to bottom left) the angle α defined in Chart I. Each division on the X axis corresponds to an increment of 0.14 Å) and the first division corresponds to R = 1.86 Å. Each division on the Y axis corresponds to an increment of 3.0° and the first division corresponds to $\alpha \approx 59.0°$.

conical intersection rather than a local maximum on S_0 or a local minimum on S_1. Thus, geometry optimization on the excited-state sheet crosses onto the ground-state sheet for a small change in geometric variables. On the ground-state sheet, for a small change in the variable α, the force changes from a large positive value to a large negative value.

The conical intersection that we have just discussed has an analogy in a crossing that is allowed by symmetry in H_4 and has been carefully studied by Gerhartz, Poshusta, and Michl.[11] Gerhartz, Poshusta, and Michl studied triply right tetrahedral C_{2v} geometries of H_4 for the A_1/A_2 states that are analogous to the S_0/S_1 states encountered in the $2_s + 2_s$ cycloaddition studied

(11) Gerhartz, W.; Poshusta, R. D.; Michl, J. *J. Am. Chem. Soc.* **1977**, *99*, 4263.

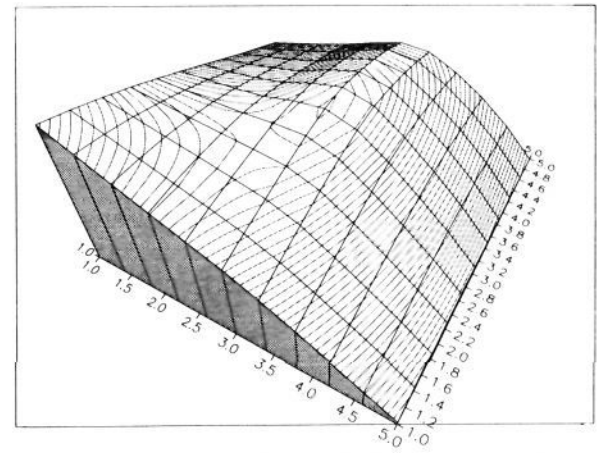

Figure 8. Potential energy surface obtained by using the MC-SCF method at the 4-31G level for the ground state (S_0) 2 + 2 cycloaddition of two ethylene molecules. The grid is the same as in figure 7.

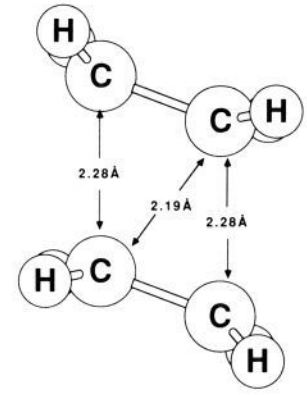

Figure 9. Geometry of the apex of the double cone for the 2 + 2 cycloaddition of two ethylene molecules computed at the MC-SCF 4-31G level.

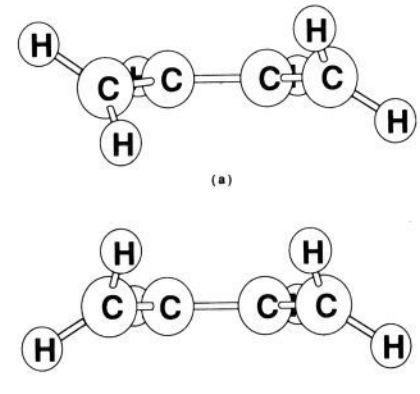

Figure 10. Scale drawings of the geometries of the "transition" states for the (a) allowed conrotatory mechanism and (b) forbidden disrotatory mechanism. The transition state for the disrotatory mechanism is in fact a local maximum with two negative directions of curvature in the Hessian.

here. When the methylene groups are replaced by H atoms, then the structures shown in Figure 1a and b have symmetry C_{2v}. As described by Gerhartz, Poshusta, and Michl, both of these structures can be derived by distortion of H_4 from a T_d geometry where the A_1/A_2 states belong to the degenerate E representation and thus the A_1/A_2 intersection can be mapped out. (Keating and Mead[5h] have considered conical intersections in this way from a general point of view.) However, in the case of the $2_s + 2_s$ cycloaddition of two ethylenes, the structure shown in Figure 1a

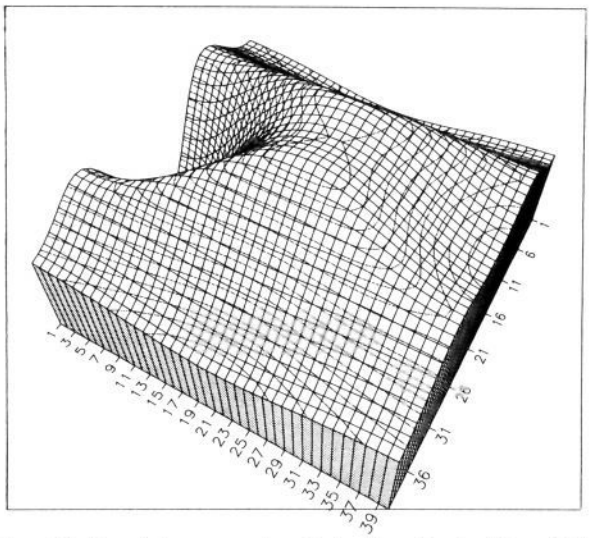

Figure 11. Potential energy surface obtained by using the VB model for the ground-state (S_0) electrocyclic reaction of cis-butadiene. The X axis (diagonal top left to bottom right) is rotational angle (γ) about the central CC bond in *cis*-butadiene and the Y axis (diagonal top right to bottom left) is the angle of rotation (α) of the terminal methylene groups. Each division on the X axis corresponds to an increment of 4.5° and the first division corresponds to 0.0°. Each division on the Y axis corresponds to an increment of 4.5° and the first division corresponds to −90.0°. Thus, the origin is *cis*-butadiene. The values of the remaining geometrical parameters have been interpolated.

or 9 has symmetry C_{2h} (i.e., the σ_v planes are lost because of the methylene H atoms) and the two states belong to the same A_{1g} representation.

III. The Electrocyclic Reaction of *cis*-Butadiene

The scale drawings of the geometry of the conrotatory allowed and disrotatory forbidden transition structures, as determined by Breulet and Schaefer,[12] are given in Figure 10. In ref 12 accurate MC-SCF computations show that the conrotatory allowed structure is a true transition state but the disrotatory forbidden structure is a local maximum with two imaginary vibrational frequencies. For the electrocyclic reaction, the condition for eq 10 and 11 to hold is rather obvious and follows immediately from our considerations for the 2 + 2 reaction. In Scheme III we give a representation of the four orbitals in a fashion that is analogous to Scheme II. With this definition, we have the same definitions of K_R, K_P, and K_X as before. Qualitatively, for the conrotatory transition structure, K_R might be approximately equal to K_P (i.e., the π bonds to the terminal methylenes are partly broken and the middle π bond and the new σ bond are partly formed), but K_X must surely be very small so that the condition of eq 10 cannot be met. For the disrotatory transition structure (which is actually a local maximum), the new π bond is almost completely formed and all the other bonds are completely broken. Thus, KP will be large but K_R and K_X will be almost zero so that again the condition of eq 10 cannot be met. However, if we take two ethylene molecules and twist them by 90° about the CC double bond, we obviously break the double bond and so K_R goes to zero. Thus, for the ethylene + ethylene reaction there is an obvious point where the condition of eq 10 is met, namely, at infinite interfragment separation where K_P also goes to zero. However, the only difference in the electrocyclic reaction occurs in the σ frame, which enters in Q. Thus, while this situation is of no interest for two ethylenes (i.e., would correspond to the singlet–triplet crossing of an isolated ethylene reaction), for the electrocyclic reaction this situation can be realized by taking the transition structure for either the conrotatory or disrotatory transition structure and

(12) Breulet, J.; Schaefer, H. F. *J. Am. Chem. Soc.* **1984**, *106*, 1221.

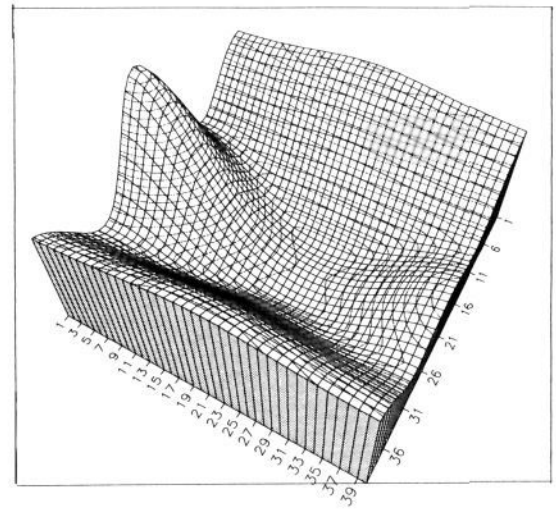

Figure 12. Potential energy surface obtained by using the VB model for the excited-state (S_1) electrocyclic reaction of *cis*-butadiene. The X and Y axes are defined as in Figure 11.

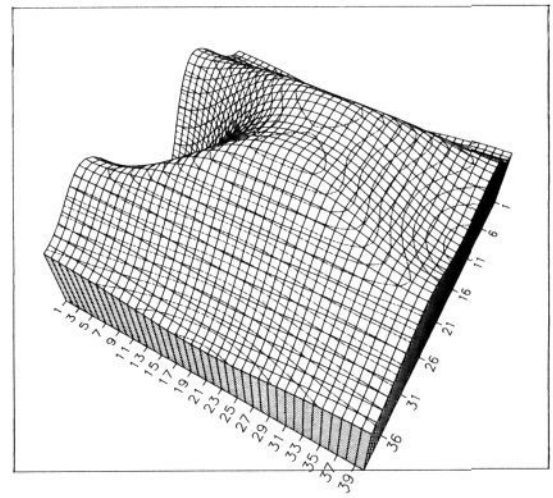

Figure 13. Potential energy surface of −T (eq 9) obtained by using the VB model for electrocyclic reaction of *cis*-butadiene. The X and Y axes are defined as in Figure 11.

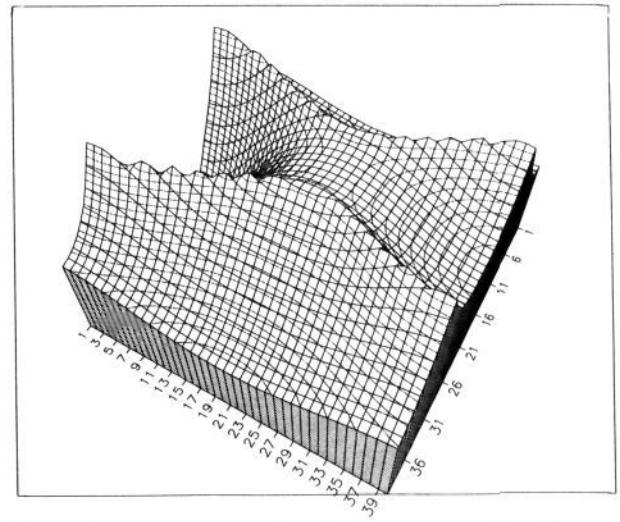

Figure 14. Potential energy surface of the lowest energy sheet of α_R and α_P as defined in eq 6a/6b obtained by using the VB model for electrocyclic reaction of *cis*-butadiene. The X and Y axes are defined as in Figure 11.

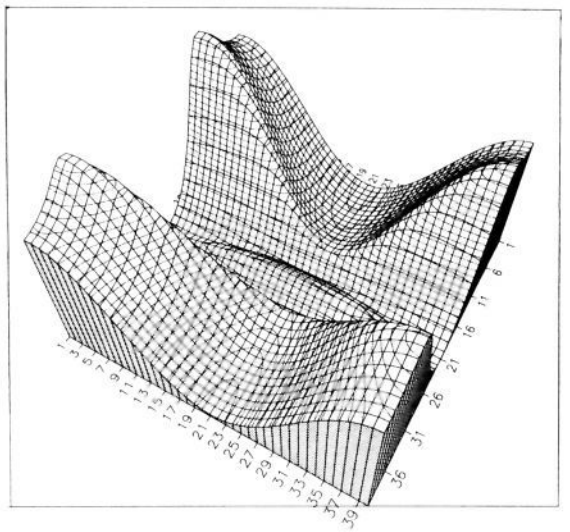

Figure 15. Potential energy surface for $|\beta|$, the resonance energy, obtained by using the VB model for electrocyclic reaction of *cis*-butadiene. The X and Y axes are defined as in Figure 11.

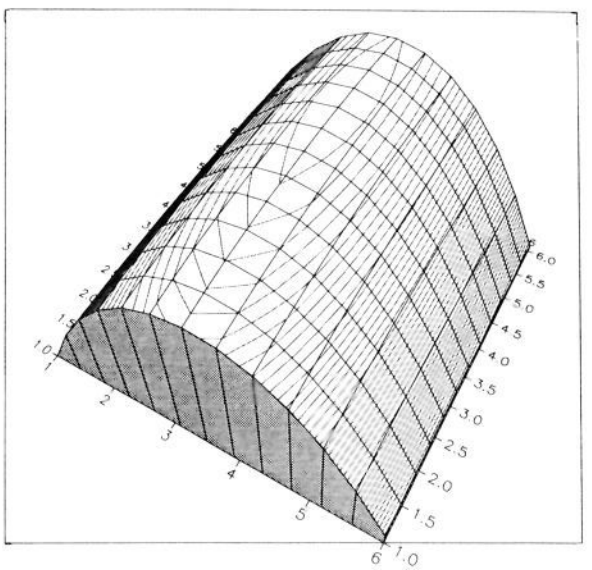

Figure 16. Potential energy surface obtained by using the MC-SCF method at the STO 3G level for electrocyclic reaction of *cis*-butadiene. The X axis (diagonal top left to bottom right) is the rotational angle about the central CC bond in *cis*-butadiene and the Y axis (diagonal top right to bottom left) is the angle of conrotation of the terminal methylene groups. Each division on the X axis corresponds to an increment of 4.0° and the first division corresponds to 70.0°. Each division on the Y axis corresponds to an increment of 1.4° and the first division corresponds to 83° (i.e., 0° corresponds to the orientation of the terminal methylenes in planar *cis*-butadiene).

Scheme III

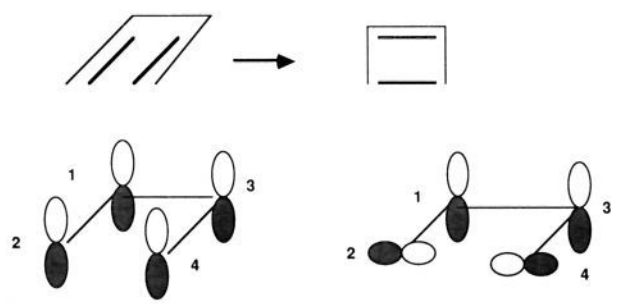

rotating by 90° about the central CC bond. This would set both K_{13} and K_{24} to zero. Thus, for the electrocyclic reaction we satisfy

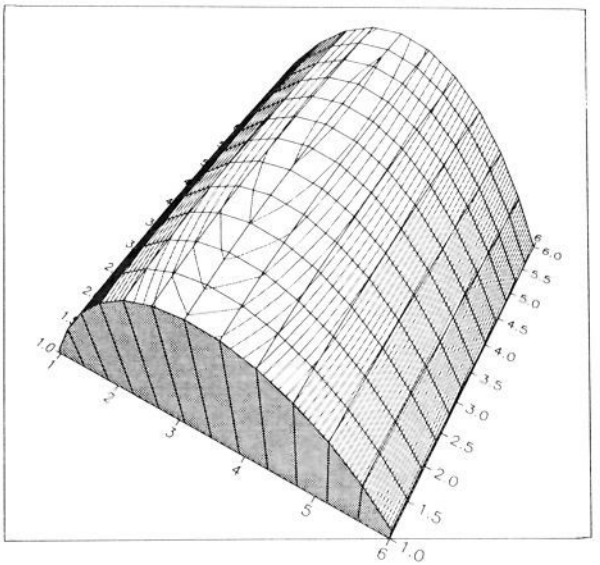

Figure 17. Potential energy surface obtained by using the MC-SCF method at the 4-31G level for electrocyclic reaction of *cis*-butadiene. The grid is the same as in Figure 16.

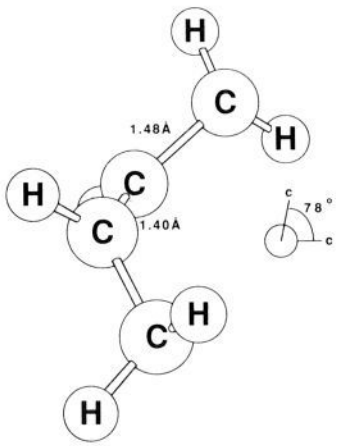

Figure 18. Geometry of the apex of the double cone for the electrocyclic reaction of *cis*-butadiene computed at the MC-SCF 4-31G level.

the condition for the double cone when $K_R = K_P = K_X = 0$.

We now give the evidence for the existence of the double cone condition in the same manner as for the 2 + 2 reaction. In Figures 11 and 12 we show the ground and excited surfaces obtained in the same manner as the data in Figures 2 and 3. The X axis (top left to bottom right) corresponds to rotation about the central CC bond in *cis*-butadiene. The Y axis (bottom left to top right) corresponds to the rotation of the terminal methylenes. The distance between the terminal methylene groups has been interpolated along the Y coordinate. Again the Y axis is symmetric. For the electrocyclic reaction, *cis*-butadiene corresponds to X approximately zero on the left of the figure while the right side of the figure corresponds to *trans*-butadiene. We again see a pair of double cones in Figures 11 and 12 (corresponding to a rotation about the central CC bond of approximately 90°. The apex is rather flat simply because the K_{ij} change only very slowly in the region where the individual $K_{ij} = 0$ (i.e., $-T = 0$ in this case because all the K_{ij} go to 0 simultaneously). This can be seen clearly in Figure 13 where we have plotted $-T$. Notice the flat maxima in $-T$ that occur at the same position as the corresponding features in Figure 11. The conditions given in eq 11a,b are shown in Figure 14 (note the ridge corresponding to conditions given in eq 11a) and in Figure 15 (note the pair of valleys in the region of α = 0° that correspond to eq 11b). Finally, in Figures 16 and 17 we show the data for the ground-state potential energy surface computed from the MC-SCF grid. Again, these results confirm

the existence of the double cone. The geometry of the apex of the cone is shown in Figure 18. Note that because of the torsional angles, all the π bonds are completely broken.

IV. Conclusions

In this work we have demonstrated the existence of real conical intersections on the potential surfaces for two "textbook" pericyclic reactions. While we have found only one point on the $n - 2$ dimensional hyperline, this demonstrates that such topological features do exist.

The common assumption in organic photochemistry is that one of the central features in the mechanism of an excited-state pericyclic reaction is the existence of an avoided surface crossing the allows for the occurrence of a radiationless jump from S_1 to S_0, which is controlled by the gap between S_1 to S_0. On the other hand, the role of conical intersections on the rate of intersystem crossing seems to be widely recognized by dynamicists. Thus, a reaction that starts out on S_1 may cross directly to the ground-state surface via the conical intersection and thus the mechanism is controlled not by the S_1 to S_0 gap but rather by the presence of minima and transition states on S_0 and S_1 themselves. For the 2 + 2 cycloaddition reaction considered in this work, the biradicaloid structure on the excited-state surface is not a minimum at all but rather a transition structure with a transition vector that points to the upper part of the double cone (where return to S_0 is fully efficient). Similarly, on the S_1 surface for the electrocyclic reaction of butadiene, at the geometry of the transition state for the ground-state reaction, there is a downhill direction leading again to a conical intersection. Thus, on the S_1 surface, for geometries in the region of ground transition structures, the crossing is indeed avoided; however, a real crossing occurs at other geometries that can be predicted qualitatively by using eq 10.

Acknowledgment. This work was supported (in part) by the Science and Engineering Research Council (UK) under Grant GR/F/48029 and GR/E/4499.4.

Registry No. Ethylene, 74-85-1; *cis*-butadiene, 106-99-0.

Molecular Dynamics Simulation of a Dilute Aqueous Solution of Benzene

Per Linse

Contribution from Physical Chemistry 1, Chemical Center, University of Lund, P.O. Box 124, S-221 00 Lund, Sweden. *Received June 20, 1989*

Abstract: A dilute aqueous solution of benzene has been investigated by means of molecular dynamics simulations. The obtained preferential orientation of water molecules in the first hydration shell of benzene due to the aromaticity confirms previous results performed with different water potentials. Despite the preferential water orientation, the hydrogen-bonded network is enforced, as typically found for hydration of apolar solutes. The translational motion of benzene is slowed down by 25% and the anisotropic reorientational motion is increased 4 times as compared to pure benzene as a consequence of a more rigid and compressed oblate cage formed by the surrounding water molecules.

The generally accepted picture of hydrophobic hydration, arising both from experiment and from computer simulation, is that the loose network of hydrogen bonds is strengthened around the nonpolar solute, giving a more ordered water structure.[1-3] On the other hand, the interaction between an ion and water is quite different. The prevalent picture of ions in aqueous solutions stems from the work of Gurney[4] and Frank and Wen.[5] In this case, the orientation of water molecules close to the ion is goverened by the ion–water interaction, and the network of hydrogen bonds is partially destroyed.

A wealth of detailed information on the structure of water around a nonpolar solute molecule and the dynamics has been provided by Monte Carlo (MC) and molecular dynamics (MD) techniques. The interest spans the whole range from small, often spherical, solutes to more complex molecules such as fragments of biomolecules.[6-14] The aqueous hydration of benzene is of special interest since the typical hydrophobic hydration of apolar species may be altered by the presence of the aromaticity. The hydration of benzene is also of relevance for the hydration of other unsaturated ring structures, as in some amino acids and the nucleotide bases.

Dilute aqueous solutions of benzene have been the subject of investigations by Ravishanker, Mehrota, Mezei, and Beveridge[12] and by Linse, Karlström, and Jönsson.[11] The same water but different benzene–water potentials were used in these studies, and since MC technique was employed, only static information was provided. The results showed that the benzene was surrounded by a primary hydration shell of ≈23 water molecules. Ravishanker et al.[12] concluded that the hydration of benzene is consistent with that found for alkanes except for two water molecules, one on each side of the benzene plane, which showed a weak hydrogen bond

(1) Franks, F. *Water—A Comprehensive Treatise*; Franks, F., Ed.; Plenum Press: New York, 1972; Vol. 2.
(2) Ben-Naim, A. *Water and Aqueous Solutions*; Plenum Press: New York, 1972.
(3) Tanford, C. *The Hydrophobic Effect*, 2nd ed.; Wiley: New York, 1980.
(4) Gurney, R. W. *Ionic Process in Solutions*; McGray-Hill: New York, 1953.
(5) Frank, H. S.; Wen W. Y. *Discuss. Faraday Soc.* **1957**, *24*, 133.
(6) Swaminathan, S.; Harrison, S. W.; Beveridge, D. L. *J. Am. Chem. Soc.* **1978**, *100*, 5705.
(7) Geiger, A.; Rahman, A.; Stillinger, F. H. *J. Chem. Phys.* **1979**, *70*, 263.
(8) Geiger, A. *Ber. Bunsenges. Phys. Chem.* **1981**, *85*, 52.
(9) Alagona, G.; Tani, A. *J. Chem. Phys.* **1980**, *72*, 580.
(10) Jorgensen, W. L. *J. Chem. Phys.* **1982**, *77*, 5757.
(11) Linse, P.; Karlström, G.; Jönsson, B. *J. Am. Chem. Soc.* **1984**, *106*, 4096.
(12) Ravishanker, G.; Mehrotra, P. K.; Mezei, M.; Beveridge, D. L. *J. Am. Chem. Soc.* **1984**, *106*, 4102.
(13) Belch, A. C.; Berkowitz, M.; McCammon, J. A. *J. Am. Chem. Soc.* **1986**, *108*, 1755.
(14) Maliniak, A.; Laaksonen, A.; Korppi-Tommola, J. *J. Am. Chem. Soc.* **1990**, *112*, 86, and references citated therein.

0002-7863/90/1512-1744$02.50/0